



Deposited via The University of Leeds.

White Rose Research Online URL for this paper:

<https://eprints.whiterose.ac.uk/id/eprint/98618/>

Version: Accepted Version

Proceedings Paper:

Wareing, CJ, Fairweather, M, Woolley, RM et al. (2015) Comparison of Numerical Predictions with CO2 Pipeline Release Datasets of Relevance to Carbon Capture and Storage Applications. In: AIP Conference Proceedings. 11th International Conference of Computational Methods in Sciences and Engineering (ICCMSE 2015), 20-23 Mar 2015, Athens, Greece. American Institute of Physics (AIP). Article no: 080004. ISSN: 0094-243X. EISSN: 1551-7616.

<https://doi.org/10.1063/1.4938799>

Reuse

Items deposited in White Rose Research Online are protected by copyright, with all rights reserved unless indicated otherwise. They may be downloaded and/or printed for private study, or other acts as permitted by national copyright laws. The publisher or other rights holders may allow further reproduction and re-use of the full text version. This is indicated by the licence information on the White Rose Research Online record for the item.

Takedown

If you consider content in White Rose Research Online to be in breach of UK law, please notify us by emailing eprints@whiterose.ac.uk including the URL of the record and the reason for the withdrawal request.

Comparison of Numerical Predictions with CO₂ Pipeline Release Datasets of Relevance to Carbon Capture and Storage Applications

Christopher J. Wareing^{a,b}, Michael Fairweather^a, Robert M. Woolley^a,
and S.A.E.G. Falle^c

^a*School of Chemical and Process Engineering, University of Leeds, Leeds, LS2 9JT, U.K.*

^b*School of Physics and Astronomy, University of Leeds, Leeds, LS2 9JT, U.K.*

^c*School of Mathematics, University of Leeds, Leeds, LS2 9JT, U.K.*

Abstract. Predicting the correct multi-phase fluid flow behaviour during the discharge process in the near-field of sonic CO₂ jets is of particular importance in assessing the risks associated with transport aspects of carbon capture and storage schemes, given the very different hazard profiles of CO₂ in the gaseous and solid states. In this paper, we apply our state-of-the-art mathematical model implemented in an efficient computational method to available data. Compared to previous applications, an improved equation of state is used. We also compare to all the available data, rather than just subsets as previously, and demonstrate both the improved performance of the fluid flow model and the variation between the available datasets. The condensed phase fraction at the vent, puncture or rupture release point is revealed to be of key importance in understanding the near-field dispersion of sonic CO₂.

Keywords: Complex Fluids, Computational Fluid Dynamics, Multi-phase Flow

PACS: 02.60.Cb, 47.40.Hg, 47.55.Ca, 47.55.Kf, 64.30.-t

INTRODUCTION

Carbon capture and storage (CCS) refers to a set of technologies designed to reduce carbon dioxide (CO₂) emissions from large point sources of emission such as coal-fired power stations, in order mitigate greenhouse gas production. CCS technology, or sequestration, involves capturing CO₂ and then storing it in a reservoir, instead of allowing its release to the atmosphere, where it contributes to climate change. Necessary transportation can be achieved in different ways, but it is commonly acknowledged that high pressure pipelines transporting liquid CO₂ will be the most reliable and cost effective choice. Their safe operation is of paramount importance as the inventory would likely be several thousand tonnes and CO₂ poses a number of dangers upon release due to its physical properties; it is a colourless, odourless asphyxiant which sinks in air and has a tendency to solid formation upon release with subsequent sublimation. It has a toxic effect in inhaled air at concentrations around 5% and causes hyperventilation above 2% [1, 2].

A number of projects have included experiments investigating the behaviour of high pressure CO₂ releases simulating accidental or operational CCS scenarios. Typically these are dense phase pure CO₂ releases into air with varying levels of humidity. Data is available in the public domain, either published or freely downloadable, from the CO2PIPETRANS¹ and CO2PIPEHAZ² European-funded projects, from the industry-funded COOLTRANS [3, 4] research programme and from laboratory scale experiments [5].

In this paper, we perform the first overall comparison between the available datasets by employing our state-of-the-art multi-phase heterogeneous discharge and dispersion model, with an improved composite equation of state. This model is capable of predicting both near and far-field fluid dynamic and phase phenomena. Predictions are based on the solutions of the density-weighted, time-averaged forms of the transport equations for mass, momentum, and total energy. Closure of this equation set is achieved with a compressibility-corrected k- ϵ turbulence model.

¹http://www.dnv.com/industry/oil_gas/services_and_solutions/technical_advisory/process_integrity/ccs_carbon_capture_storage/co2pipetrans/Index.asp

²<http://co2pipehaz.eu/>

NUMERICAL TECHNIQUE

We have started from the numerical technique described in [6] to predict the flow. In that technique, predictions are based on Reynolds-averaged Navier-Stokes (RANS) equation solutions of the density-weighted, time-averaged (Favre) forms of the transport equations for mass, momentum and total energy. Closure of the equation set is achieved through a $k-\epsilon$ turbulence model, with added compressibility corrections [7]. As in [6], solutions are obtained of the time-dependent, axisymmetric forms of the descriptive equations and the integration of the equations performed by a shock-capturing conservative, upwind second-order accurate Godunov numerical scheme. The fully-explicit, time-accurate, cell-centred finite-volume Godunov method is a predictor-corrector procedure, where the predictor stage is spatially first-order, and used to provide an intermediate solution at the half-time step. This solution is then subsequently used at the corrector stage for the calculation of second-order accurate fluxes that lead to a second-order accurate cell-centred solution. A Harten, Lax, van Leer Riemann solver is employed to calculate fluxes at cell boundaries. The numerical scheme employs an unstructured adaptive mesh refinement technique which automatically allows for finer resolution in the regions of strong gradients and lower resolutions elsewhere. The grid is also defragmented in hardware memory on every timestep, increasing efficiency further. The scheme employs a composite numerical equation of state method for CO_2 described in [6]. This efficient thermodynamic method employs the Peng-Robinson [8] equation of state in the gas phase, and look-up tables from Span and Wagner [9] in the liquid phase. This composite approach has now been validated for free releases into air [10, 11], as well as punctures [12] and ruptures [13] of buried pipelines. In an improvement over the method in [6], tables from the Jager and Span [14] equation of state for solid CO_2 are now employed in the solid phase instead of tables from the DIPPR database.

EXPERIMENTAL DATASETS

We have obtained experimental temperature data regarding near-field releases of high pressure liquid phase CO_2 from a number of sources. These are detailed in Table 1, with the differences between tests highlighted. From each test, we have used consistent, averaged temperature measurements for comparison to the RANS predictions. Each measurement has a variance of a degree or two over this averaging period. The thermocouple sensors used to take these measurements are accurate over the observed temperature range to within $\pm 5\text{K}$ at worst. Hence throughout this analysis, we have assumed an experimental error of 5K. The plotted temperature is the simple average for that particular sensor in that particular test during the averaging period. Release diameters vary from 2.0 to 25.0mm. The majority of the releases are horizontal. Where known, the estimated liquid fraction at the nozzle varies from $\sim 80\%$ to 100%. The tests are either releases from an isolated depressurising reservoir, or from a reservoir with a driving pressure to maintain the reservoir pressure. For complete details of each experimental dataset, please consult the source of the dataset.

TABLE (1). Experimental data regarding near-field releases of high pressure liquid phase CO_2 .

Name	Release diam. (D) (mm)	Horiz./ Vert.	Reservoir Pressure (barg)	Estimated liquid fraction at nozzle (%)	Buffer/free	Source
BP Test 2	11.94	H	155	-	Buffer	CO2PIPETRANS
BP Test 5	25.62	H	157	-	Buffer	CO2PIPETRANS
BP Test 11	11.94	V	82	-	Buffer	CO2PIPETRANS
Shell Test 3	12.7	H	150	-	Buffer	CO2PIPETRANS
Shell Test 5	25.4	H	150	-	Buffer	CO2PIPETRANS
Shell Test 11	12.7	H	80	-	Buffer	CO2PIPETRANS
HSL Test C	2.0	H	54	84%	Free	[5]
HSL Test D	4.0	H	49	86%	Free	[5]
CLTRNS T7	24.3	V	150	100%	Buffer	COOLTRANS [10]
INERIS T6	9.0	H	95	$\sim 100\%$	Free	CO2PIPEHAZ [11]
INERIS T7	12.0	H	85	$\sim 100\%$	Free	CO2PIPEHAZ [11]
INERIS T8	25.0	H	77	$\sim 100\%$	Free	CO2PIPEHAZ [11]
INERIS T11	12.0	H	83	$\sim 100\%$	Free	CO2PIPEHAZ [15]
INERIS T12	25.0	H	77	$\sim 100\%$	Free	CO2PIPEHAZ [15]
INERIS T13	50.0	H	69	80-90%	Free	CO2PIPEHAZ [15]

INITIAL CONDITIONS AND COMPUTATIONAL TECHNIQUE

In order to calculate the numerical prediction, we used the initial conditions at the release point calculated in [10] for CLTRNS T7. For full details, please see [10], but important to note is that the fluid phase is 100% liquid at the release point. Three two-dimensional simulations in cylindrical polar coordinates were performed in order to obtain predictions out to 850D, the first capturing the sonic decompression and Mach shock and then the remaining domain was split between two simulations for computational efficiency. Even so, the simulations took several tens of thousands of CPU hours on the ARC high performance computing facility at the University of Leeds.

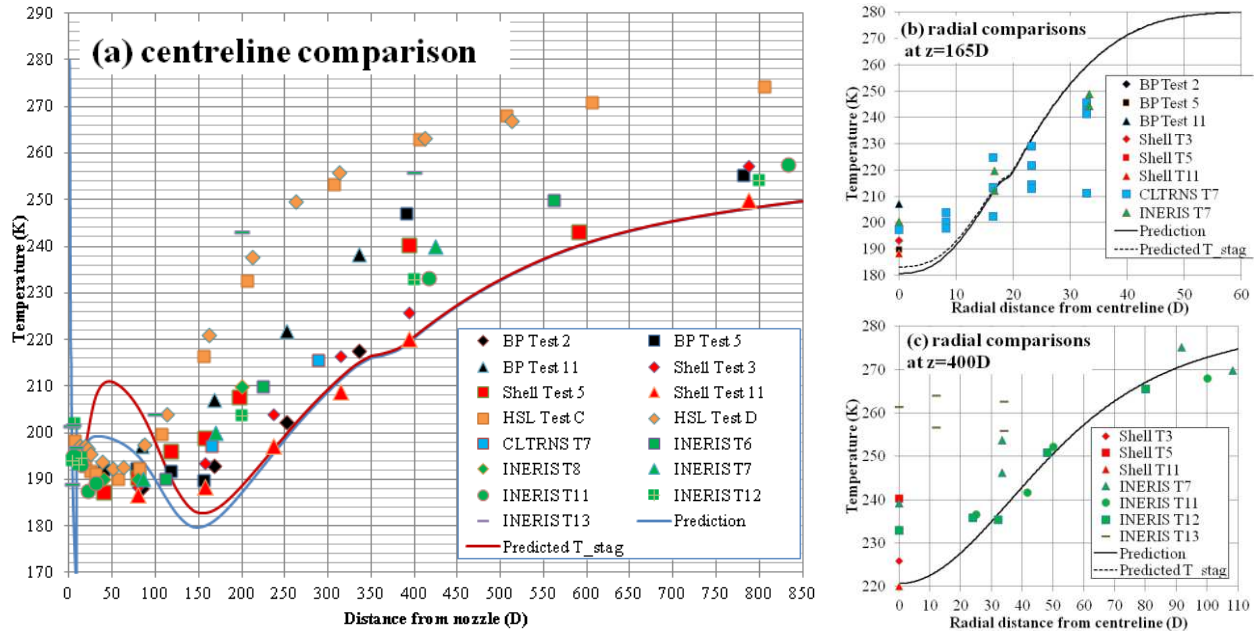


FIGURE 1. A comparison between experimental data and numerical prediction along the centreline of the jet (a) and radially at 165D (b) and 400D (c) along the centreline. The experimental data has an error of $\pm 5K$ throughout; error bars are omitted in the figure for clarity.

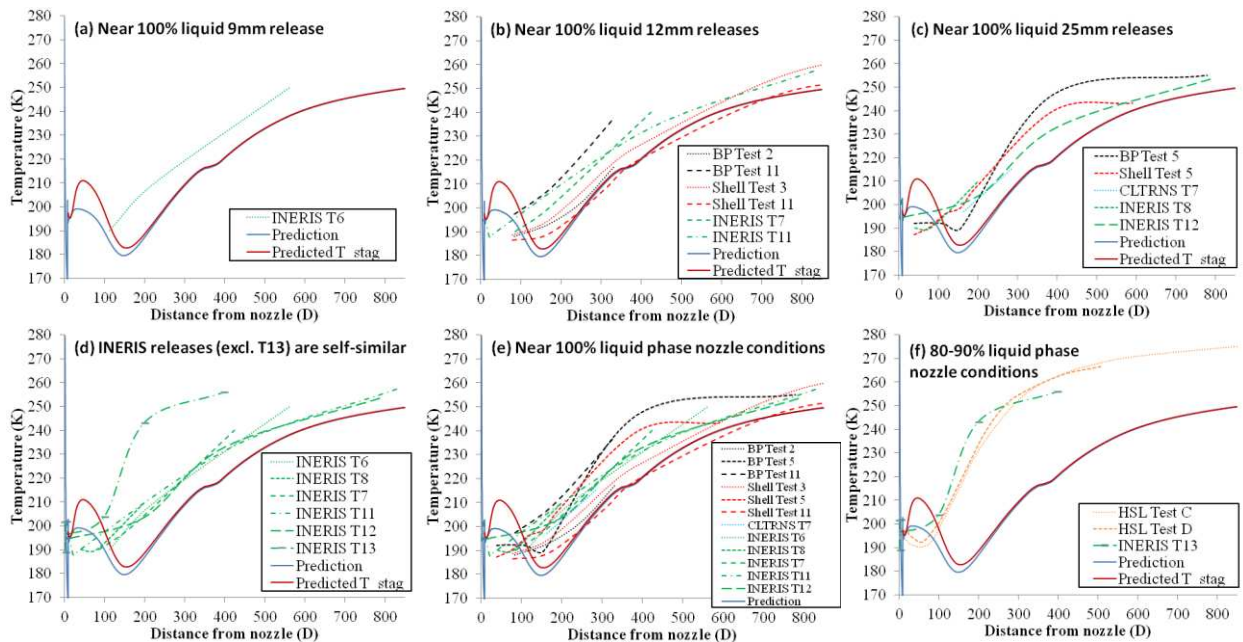


FIGURE 2. Illuminating the agreement (or not) of different subsets of the data in Figure 1 when plotted by different experimental properties: (a) $D=9\text{mm}$, (b) $D=12\text{mm}$, (c) $D=25\text{mm}$, (d) INERIS tests, (e) release point phase conditions 100% liquid and (f) 80-90% liquid phase. Dashed lines indicate experimental data, solid lines the numerical predictions.

RESULTS AND CONCLUSIONS

In Figure 1(a) we show for the first time all the available datasets on the centreline of the jet dimensionalised according to the release diameter (D). We also show the predicted centreline temperatures and stagnation temperatures stitched together from the numerical simulations. It is clear that the numerical prediction is on the colder side of the available experimental data. It is in very good agreement with some data, for example the Shell T11 where the prediction is in almost exact agreement from 200-800 D. Over this range it is also within the error of several other datasets. There is a very large spread in the data along the centreline of the jet and some datasets (e.g. HSL Test C, D and INERIS T13) warm up along the jet considerably more quickly. In Figures 1(b) and 1(c) we demonstrate for the first time agreement between numerical predictions and experimental data of the radial temperature distribution from multiple sources at 165D and 400D along the centreline. At 165D the numerical prediction would appear to be cold in the core, although within experimental error, but also too narrow compared to the data. At 400D, the prediction is in excellent agreement with several datasets, although it is immediately apparent that one dataset (INERIS T13) is not in a similar temperature range to the others shown.

In an effort to examine why there are differences between the datasets and how numerical modellers could best use each dataset in future, we have split the representation of the data according to 1) nozzle diameter with 100% liquid fraction (Figures 2(a)-2(c)), 2) INERIS data (Figure 2(d)) and 3) liquid phase fraction (Figures 2(e) and 2(f)). It is not clear that splitting according to release diameter shows any particular trend. There is only one 9mm release, and the 12 mm and 25mm releases have similar temperatures ranges in their data. This exercise does indicate that for ~100% liquid releases, the centreline temperatures are self-consistent when dimensionalised according to nozzle diameter; release diameter is not a key parameter. Figure 2(d) shows the INERIS datasets. Five out of six are self-consistent – all 100% liquid releases. The case where the liquid fraction at the nozzle was 80-90% (T13) is clearly warming along the jet much more quickly. Figures 2(e) and 2(f) highlight that the liquid fraction at the release point is the key parameter in differentiating between these datasets. The releases with ~100% liquid at the release point are reasonably well grouped together (Fig. 2(e)) and the releases with liquid fraction known to be in the range 80-90% are reasonably closely grouped together (Fig. 2(f)).

In conclusion, we have shown here for the first time that our method, with an improved equation of state, is able to model multiple datasets for sonic CO₂ decompressions from high pressure pipelines. We have also shown that there is considerable variation in the experimental data available, which can be understood in terms of the liquid fraction at the release point. A number of simulations are now planned to explore this further, with an improved second-moment Reynolds stress turbulence model. In the meantime, we hope that this novel comparison of the available data will make numerical modellers aware of the dataset differences.

ACKNOWLEDGMENTS

The numerical simulations were carried out on the STFC-funded DiRAC I UKMHD Science Consortia machine enabled through the ARC HPC resources and support team at the University of Leeds.

REFERENCES

1. S. Connolly and L. Cusco, *ICHEM Symposium Series* **153**, 1-5 (2007).
2. A.J. Wilday, A. McGillivray, P. Harper and M. Wardman, *ICHEM Symposium Series* **155**, 392-398 (2009).
3. R. Cooper, *J. Pipeline Eng.* **11**, 155-372 (2012).
4. D. Allason, K. Armstrong, P. Cleaver, A. Halford and J. Barnett, *ICHEM Symposium Series* **158**, 142-152 (2012).
5. M. Pursell, *ICHEM Symposium Series* **158**, 164-171 (2012).
6. C.J. Wareing, R.M. Woolley, M. Fairweather and S.A.E.G. Falle, *AIChE J.* **59**, 3928-3942 (2013).
7. S. Sarkar, G. Erlebacher, M. Y. Hussaini and H. O. Kreiss, *J. Fluid Mech.* **227**, 473-493 (1991).
8. D.-Y. Peng and D. B. Robinson, *Ind. Eng. Chem. Fundam.* **15**, 59-64 (1976).
9. R. Span and W. Wagner, *J. Phys. Chem. Ref. Data.* **25**, 1509-1596 (1996).
10. C.J. Wareing, M. Fairweather, S.A.E.G. Falle and R.M. Woolley, *Int. J. Greenhouse Gas Control* **20**, 254-271 (2014).
11. R.M. Woolley, M. Fairweather, C.J. Wareing, S.A.E.G. Falle, C. Proust, J Hebrard and D. Jamois, *Int. J. Greenhouse Gas Control* **18**, 139-149 (2013).
12. C.J. Wareing, M. Fairweather, S.A.E.G. Falle and R.M. Woolley, *Int. J. Greenhouse Gas Control* **29**, 231-247 (2014).
13. C.J. Wareing, M. Fairweather, S.A.E.G. Falle and R.M. Woolley, *Int. J. Greenhouse Gas Control*, accepted (2015).
14. A. Jager and R. Span, *J. Chem. Eng. Data* **57**, 590-597 (2012).
15. D. Jamois, C. Proust, J. Hebrard, and O. Gentilhomme. *Récents Progrès en Génie des Procédés*, Numéro 104 (2013).